A Fetal Movement Simulation System for Wearable Vibrational Sensors

Chenxi Yang, *Student Member, IEEE*, Negar Tavassolian, *Senior Member, IEEE*

***Abstract*—This paper introduces a low-cost phantom system that simulates fetal movements (FMVs) for the first time. This vibration system can be used for testing wearable inertial sensors which detect FMVs from the abdominal wall. The system consists of a phantom abdomen, a linear stage with a stepper motor, a tactile transducer, and control circuits. The linear stage is used to generate mechanical vibrations which are transferred to the latex abdomen. A tactile transducer is implemented to add environmental noise to the system. The system is characterized and tested using a wireless sensor. The sensor recordings are analyzed using time-frequency analysis and the results are compared to real FMVs reported in the literature. Experiments are conducted to characterize the vibration range, frequency response, and noise generation of the system. It is shown that the system is effective in simulating the vibration of fetal movements, covering the full frequency and magnitude ranges of real FMV vibrations. The noise generation test shows that the system can effectively create scenarios with different signal-to-noise ratios for FMV detection. The system can facilitate the development of fetal movement monitoring systems and algorithms.**

I. Introduction

Over 26,000 cases of stillbirth occur in the United States every year [1]. It has been shown that objective and continuous monitoring of fetal vital signs could identify fetal compromise and decrease stillbirth rates through time-sensitive management [2]. Fetal movement (FMV) is one of the vital signs that are important in monitoring stillbirth. A gradual decrease in fetal movement during the days before stillbirth has been reported by 50% of women encountering stillbirth [3]. Interventions can be conducted if the reduction in FMV is detected timely, potentially preventing the compromise of the baby [4].

FMV monitoring inside the clinic is generally performed using ultrasound imaging and fetal cardiotocography [2]. These modalities are active, constraining and not suitable for use outside of the clinic [2]. Passive methods that have been studied in FMV detection are based on acoustic [5], electric and [5], inertial modalities [6], [7]. Among them, inertial modalities reveal promising potential due to their small size, low power consumption, and convenience of use [6]. Accelerometers pick up the vibrations on the maternal abdomen caused by fetal movements. It has been shown FMVs could be recorded, detected and classified using an array of accelerometers [6]. However, there are still challenges in processing signals such as canceling motion artifacts and maternal interference [6]. Therefore, there is a considerable need for the development of FMV monitoring algorithms. A simulation system that can be used for the initial testing and validation of these algorithms would be highly beneficial. Such a system could provide various FMV conditions by simply adjusting simulation parameters rather than performing large-scale data collection from subjects. The experimental results from the simulation system could also support the approval of experiments with human subjects. The phantom could also be used for a standardized comparative evaluation of different monitors or algorithms.

In this paper, a prototype is made to simulate FMV-induced vibrations on the maternal abdominal wall. The system is built with off-the-shelf, low-cost components which make it affordable and reproducible. A wearable sensor is used to characterize and test the performance. To the best of our knowledge, this is the first vibrational simulation system which has been developed for mimicking fetal movements.

The structure of the paper is as follows. The hardware and software design of the system are introduced in Section II. The experimental setups and results are presented in Section III. Section IV summarizes the paper and discusses future work.

II. Methods

A. The Hardware System

Fig. 1 shows a detailed structure of the system. The hardware consists of three main parts. The first part is the phantom abdomen. The second part is the vibration actuator and transducer. The third part is the control circuits of the vibration. The front view of the system is demonstrated in Fig. 1 (a). The phantom abdomen, shown as part C in Fig. 1 (a), is made of a latex balloon which has a flat bottom and a curved top side. The balloon is 150 millimeter (mm) tall, 400 mm long, and 300 mm wide. It is filled with water to simulate the abdominal environment.

The balloon is located on top of the FMV vibration actuator and transducer. A linear stage (FSL40E20010C7, FUYU technology) equipped with a stepper motor (F in Fig. 1) forms the foundation of the simulator structure. The linear stage is a robotic structure that allows a metal block (A) to move horizontally with a range of 200 mm and an accuracy of 0.05 mm. The linear stage translates the rotational movement of the stepper motor into a linear motion of A. The white arrows show the direction of the movement in Fig. 1 (a). The linear stage has the capability to relocate the center of the vibration (A) to any point along its axis. This allows the system to simulate fetal movements originating from different locations inside the uterus. A tactile transducer (TT25-8, Dayton Audio), presented by block B in Fig. 1 (a), is connected to the top of block A. This transducer is used as an interface to transmit the vibration created by the linear stage to the

Chenxi Yang and Negar Tavassolian are with the Department of Electrical and Computer Engineering, Stevens Institute of Technology, Hoboken, NJ, 07030, USA (e-mail: negar.tavassolian@stevens.edu).

978-1-7281-1990-8/20/$31.00 ©2020 IEEE

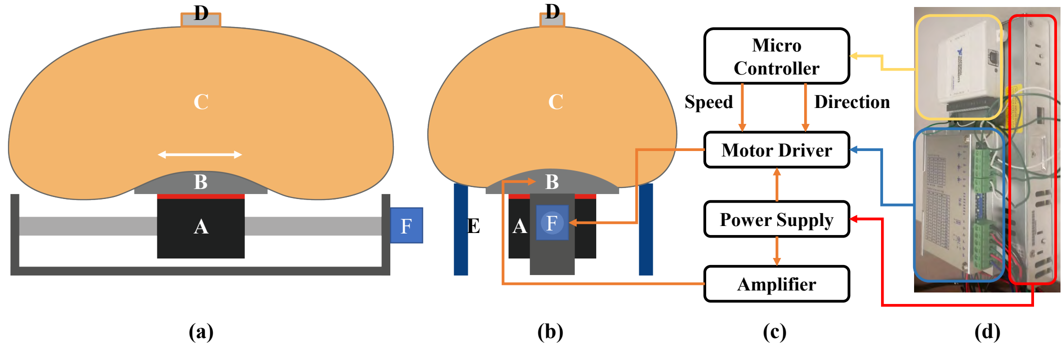

Fig. 1 (a) A front-view diagram of the system. (b) A side-view diagram of the system. (c) Diagram of the control circuits. (d) A photo of the control circuits. A: Moving block on the linear stage; B: A tactile transducer; C: The latex balloon phantom abdomen; D: An example sensor; E: Supporting material for the latex phantom; F: Stepper motor of the linear stage.

phantom. It also can generate a wide range of vibrations from 0.5 Hz to 160 Hz to simulate low-frequency environmental noise. A thin vibration insulation foam is inserted between the block (A) and the transducer (B) to attenuate the motor vibration, illustrated as the red part between A and B. Moreover, a thin layer of mineral oil is applied between the surface of the transducer (B) and the latex balloon (C) for lubrication. This lubrication alleviates the sheer noise caused by the friction between B and C.

Fig. 1 (b) shows the side view of the phantom system. In addition to the structures shown in Fig. 1 (a), two foam blocks (E) are used to support the weight of the phantom abdomen and control the position, especially the vertical height of the phantom relative to the transducer (B). The purpose of controlling the height of the phantom is to ensure a shallow interference of the transducer (B) into the flat surface of the abdomen (C). In our study, this depth represents the vertical displacement of the simulated FMV. According to literature, the displacement should be about 13-20 mm [8]. If the interference is too deep, the resulting vibration magnitude on the top surface will be too large compared to the magnitude of a real FMV.

The diagram and photo of the control circuits are presented in Fig. 1 (c) and Fig. 1 (d) respectively. The circuits in Fig. 1 (d) is enlarged (in comparison with the phantom in Fig. 1 (a)) for illustration purposes. The control system includes a stepper motor driver (FMDD50D40NOM, FUYU Inc., the blue box in Fig. 1 (d)), which is powered by a 24 V DC power supply (the red box in Fig. 1 (d)). The stepper motor driver drives the linear stage. Due to the interference between B and C, the vibration of B is transmitted through C and can be picked up by a sensor placed on the top surface of the phantom, shown by D in Fig. 1 (a). The stepper motor driver is controlled by a micro-controller (USB 6251, National Instruments), the yellow box in Fig. 1 (d). The micro-controller is programmed and operated via a laptop. The tactile transducer is driven by an audio amplifier. The environmental noise waveform is sent to the amplifier via Bluetooth from the laptop.

B. The Software Method

The software is used to control the motion of block (A) on the linear stage by sending control signals to the motor driver via the micro-controller. The control signals are two sequences of digital pulses (5 V as high, 0 V as low). One pulse sequence controls the rotation speed and the other controls the direction of the stepper motor. Our target is to control the frequency and acceleration magnitude of the vibration of the phantom abdominal wall such that they are close to the pattern of an actual FMV. Since the sensing elements are accelerometers, the vibration signals are recorded as acceleration values. According to literature, fetal movement components are below 25 Hz in frequency [6]. Their magnitudes may vary from 0.015 gravity (G) to 0.06 G as measured by accelerometers [6]. To achieve these two conditions, we configure two parameters as below.

The first parameter is the direction parameter, denoted as $\boldsymbol{D}$. This parameter is the frequency of the direction-control pulse in the unit of Hz. The motor rotates clockwise when the direction-control pulse is set to high and counterclockwise when the pulse is set to low. The block on the linear stage moves back and forth when the motor is turned clockwise and counterclockwise repetitively. Therefore, this block will vibrate at the same frequency as the control parameter $\boldsymbol{D}$. The second parameter is the step parameter, denoted as $\boldsymbol{S}$. $\boldsymbol{S}$ is the frequency of the speed-control pulse. The stepper motor rotates in steps, the minimum rotation in degrees that the motor can achieve. Every time the speed-control pulse is set from low to high, the stepper motor rotates one step. The step parameter $\boldsymbol{S}$ sets how many steps are taken per second. The rotation speed ω of the motor is defined as below.

$$\omega = S \times \frac{2\pi}{P}\ rad/s \tag{1}$$

In (1), $\boldsymbol{S}$ is the step parameter, which is in the unit of steps/second to avoid confusion with the vibration frequency in the unit of Hz. $\boldsymbol{P}$ is the motor driver configuration parameter that defines the number of steps needed to finish one revolution (rev), i.e., a full circle of rotation. This parameter can be changed by configuring the stepper motor driver and is set to 5000 steps/rev in this work. Taking the derivative of both sides of (1), the angular acceleration α could be presented as:

$$\alpha = \frac{\Delta s}{\Delta t} \times \frac{2\pi}{P} \tag{2}$$

Using the linear stage, the angular acceleration is then converted to linear acceleration a as below [9].

$$a = \frac{\alpha L}{2\pi} = \frac{\Delta S}{\Delta t} \times \frac{L}{P} \tag{3}$$

In (3), L is the lead of the linear stage, which is the linear travel distance of the block during one revolution of the motor. In this system, L is a constant parameter of 4 mm/rev. Therefore, the acceleration a has a linear relationship with the derivative of the step parameter ***S***. According to the frequency response of the motor driver [9], the angular acceleration can be approximated by:

$$\frac{\Delta S}{\Delta t} = kS \text{ when } S \ll 10P \quad (4)$$

k is a constant parameter, calculated from the moment of inertia of the system. Therefore, there is a direct linear control between linear acceleration and the step parameter ***S*** when the step parameter is much smaller than 10×P, which is 50000 steps/s in our study. The magnitude of the acceleration should change linearly for very small ***S*** values, and gradually becomes non-linear as ***S*** increases.

In summary, we control the vibration with two sequences of control parameters. The first sequence, ***D*(*t*)**, controls the frequency of the vibration along time. The second sequence, ***S*(*t*)**, controls the magnitude of the vibration. We conducted different experiments to characterize the simulation system, as shown in the following section.

III. Experimental Setups and Results

A. *Experimental Setup and Steps*

A wearable sensor node (Shimmer 3, Shimmer Sensing) represented by location D in Fig. 1 (a) is used to measure the vibration of the phantom. The sensor is attached to the top of the latex abdomen using a Tegaderm Film (1626W, 3M). The sensor is equipped with a 3-axis accelerometer, which records vibrations at a sampling frequency of 256 Hz. The data are sent to a laptop via Bluetooth and imported into MATLAB for further processing. The raw signals from the 3 axes are combined by summing the power of the three signals and then taking the square root of the sum. The combined waveforms are analyzed using continuous wavelet transform (CWT). The CWT is based on a Morse wavelet. More details of the CWT method used can be found in [10]. In addition, the envelopes of the acceleration waveforms are extracted using a peak detection algorithm with a sliding window of 256 samples. The envelopes represent the magnitude of the vibrations.

Three experiments are conducted. Firstly, the magnitudes of the vibration signals are evaluated in terms of linearity and range. We change the magnitude of vibration while keeping its frequency constant. Secondly, we evaluate the capability of covering the full range of vibration frequencies by controlling the magnitude and sweeping the frequency of the vibration. Lastly, we test the capability of producing environmental noise in the system.

1) *Magnitude Sweeping Experiment*

In this work, the repeating frequency of the vibration is set to 10 Hz, which is a representative number within the FMV range [6]. The step parameter sweeps from 250 steps/second to 10000 steps/second in 1 minute. The sweep is repeated ten times. Then the recorded vibration waveforms are ensemble-averaged to reject random noise. The CWT and envelope are generated from the outputs. The envelope of the ensembled magnitude waveforms is fitted with linear and non-linear models to analyze its linearity.

2) *Frequency Sweeping Experiment*

The step parameter is set to a constant value of 1000 steps/second. The parameter ***D*** is swept from 0.1 Hz to 25 Hz. The sweep lasts for 1 minute and is repeated ten times. Similar to Experiment 1 in the previous part, the waveforms are ensemble-averaged on the ten times of sweeping. The CWT and envelope of the recordings are extracted for analysis.

3) *Simulation of FMVs with/without Background Noise*

First, a noise-free simulation segment was designed with periodic FMVs. The segment has FMVs with durations of 2.5 seconds which repeat every 5 seconds and center frequencies of 15 Hz. The segment length is 30 seconds. The duration of 2.5 seconds is the representative length of a limb-related FMV [8]. The step parameter is set to 1000 steps/second during the simulation. Next, a noise waveform was generated by controlling the tactile transducer. The noise waveform is a random noise from 5 Hz to 25 Hz which represents the existence of maternal organ vibration and environmental vibration [6]. Five tests with different noise levels are conducted. The noise levels are controlled by configuring the gain of the audio amplifier to 2, 4, 6, 8, and 10 (times of amplification), respectively. Each test continues for 30 seconds with the same vibration parameter configuration as the noise-free segment. The signal-to-noise ratios of the FMV segments are analyzed using CWT. The signal-to-noise ratio (SNR) of the signal is defined as below.

$$SNR = 10log_{10}(\sum cwt^2{}_{signal} / \sum cwt^2{}_{noise}) \quad (5)$$

where cwt_{signal} are the CWT coefficients of the noise-free signal, and cwt_{noise} are the CWT coefficients of the noise.

B. *Experimental Results*

1) *Magnitude Sweeping Experiment*

Fig. 2 shows the results of time-frequency analysis and the relationship between the magnitude and the step parameter. Fig. 2 (a) illustrates the power of the CWT coefficients in a heatmap, demonstrating the dominant components in the time-frequency domain. It can be visually observed that the dominant frequency is centered at 10 Hz, presented by yellow

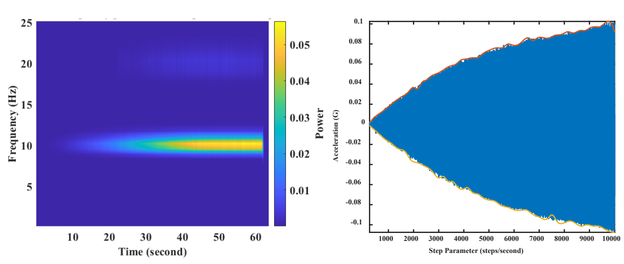

Fig. 2. (a) Time-frequency heatmap of the magnitude sweeping experiment at a vibration frequency of 10 Hz. (b) The magnitude-step plot and the envelope of the response.

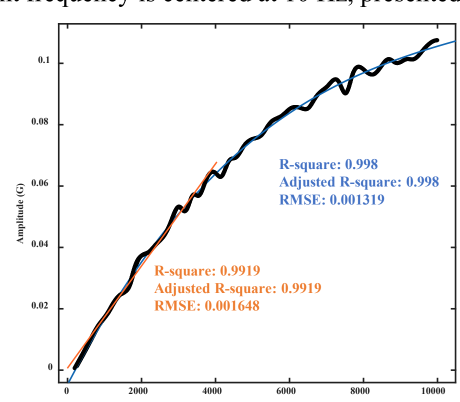

Fig. 3. Curve-fitting results of the magnitude vs. step parameter plot. Blue: fitting the full curve from 250 to 10000 steps/s. Orange: fitting the partial curve from 250 to 4000 steps/s.

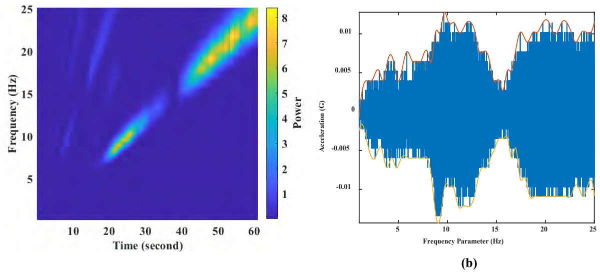

Fig. 4. (a) The time-frequency heatmap of the frequency sweeping experiment from 0.1-25 Hz with a step parameter of 1000 steps/second. (b) The magnitude-frequency plot and the envelope of the plot.

color. The power of the CWT coefficient increases during the sweeping, suggesting that the vibration frequency is kept constant during the increase of the vibration magnitude. The acceleration magnitude and its relationship with step parameter $\boldsymbol{S}$ are presented in Fig. 2 (b). It is shown that the magnitude ranges from 0.001 G to 0.1 G, fully covering the range corresponding to real fetal movement, which is from 0.015 G to 0.06 G as reported in [6].

We performed two curve-fitting procedures based on the envelope of the waveform. The first is a full-range curve-fitting from 250 to 10000 steps/second. The second is a partial curve-fitting that excludes the magnitudes which are higher than the maximum value of 0.06 G, which is from 250 to 4000 steps/second. The curve-fitting results are presented in Fig. 3. The full curve is fitted with a 3rd order polynomial, suggesting a non-linear behavior with an adjusted R-square value of 0.998 and a root-mean-square-error (RMSE) of 0.0013. We fitted a linear model to the full curve, and the R-square value is 0.945 with RMSE of 0.0069, indicating poor linearity in this case. However, the partial linear-fitting of the curve reports an R-square value of 0.9919 with RMSE of 0.0016. This result shows that the system is linear in the range needed for FMV simulations, facilitating the simulation of any FMV pattern in the magnitude aspect.

2) *Frequency Sweeping Experiment*

Fig. 4 summarizes the results of the frequency-sweeping experiment. It can be observed that the dominant frequency shifts from lower to higher frequencies with time. However, the power of the center frequency is weaker below 5 Hz and between 13 and 17 Hz as compared to the other frequency bins. A discontinued yellow strip from 5 Hz to 25 Hz along the diagonal direction of Fig. 4 (a) is observed due to the attenuation of the CWT power, which can also be observed in the time domain from the envelope in Fig. 4 (b). The results reveal that the system has a non-constant frequency response to the vibration frequency. The attenuation in magnitude below 5 Hz is caused by the starting friction of the linear stage and the attenuation between 13 and 17 Hz should be caused by the natural resonance frequency of the linear stage [9]. The attenuation of the magnitude could be compensated by linearly increasing the step parameter, as shown in Experiment 1).

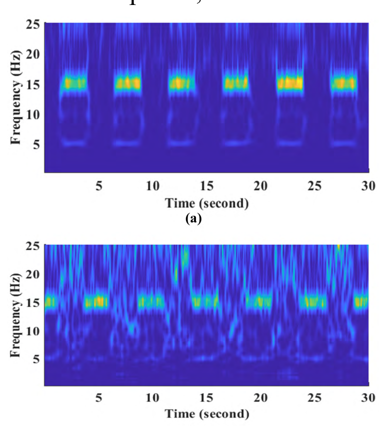

Fig. 5. Time-frequency heatmaps of: (a) the noise-free FMV segment and (b) the noisy FMV segment.

3) *Simulation of FMVs with/without Background Noise*

The CWT heatmaps of the FMV segments with and without a background noise of 6 times of amplification are presented in Fig. 5. It can be observed in Fig. 5 (a) that the noise-free segment has a clear periodic FMV pattern with a duration of 2.5 seconds. In comparison, the noisy segment is corrupted with a wide range of noise components from 5 to 25 Hz, as illustrated in Fig. 5 (b). The SNR of the noise-free measurement is 27.3 dB. In comparison, the SNR of Fig. 5 (b) is 1.9 dB. The SNR with 2, 4, 8, and 10 times of amplification in noise waveform report 24.0, 9.59, -9.4, and -22.7 dB respectively. It is shown that the system can effectively create FMVs with different signal-to-noise ratios to test the robustness of FMV detection algorithms.

IV. CONCLUSION AND FUTURE WORK

This paper presents a vibrational simulation system for simulating fetal movements for the first time. The capability of the system to generate vibrations with similar frequency and magnitude specifications as natural fetal movements was verified. The system has a linear magnitude control and a non-linear frequency response. Future work includes implementing an adaptive magnitude compensation system that improves the consistency of vibration magnitudes when changing the vibration frequency. A second linear stage can also be added to extend the vibration into two dimensions as well as locate the vibration source at any point below the phantom abdomen.

REFERENCES

[1] M. F. MacDorman, *et al,* "Fetal and Perinatal Mortality, United States, 2006," *National vital statistics reports: from the Centers for Disease Control and Prevention*, vol. 60, pp.1-22, 2012.

[2] Rebecca Brown, *et al.* "Continuous Objective Recording of Fetal Heart Rate and Fetal Movements Could Reliably Identify Fetal Compromise, Which Could Reduce Stillbirth Rates by Facilitating Timely Management," *Medical hypotheses*, no. 3, pp. 410-417, 2014.

[3] J. F. Froen, *et al.*, "Restricted fetal growth in sudden intrauterine unexplained death," *Acta Obstet. Gynecol. Scand.*, vol. 83, pp. 801–807, 2004.

[4] C. Serena, *et al.*, "Stillbirth and fetal growth restriction," *J. Matern.-Fetal Neonatal Med.*, vol. 26, no. 1, pp. 16–20, 2013.

[5] K. Nishihara, *et al.*, "A Long-Term Monitoring of Fetal Movement at Home Using A Newly Developed Sensor: An Introduction of Maternal Micro-Arousals Evoked by Fetal Movement During Maternal Sleep," *Early Hum. Dev.*, vol. 84, pp. 595–603, 2008.

[6] B. Boashash, *et al.* "Passive Detection of Accelerometer-Recorded Fetal Movements Using A Time–Frequency Signal Processing Approach," *Digital Signal Processing*, vol. 25, pp: 134-155, 2014.

[7] M. Altini, *et al.* "Detection of Fetal Kicks Using Body-Worn Accelerometers During Pregnancy: Trade-Offs Between Sensors Number and Positioning," *In Eng. in Med. and Bio. Soci. (EMBC), 2016 IEEE 38th Ann. Int. Conf. of the*, pp. 5319-5322., 2016.

[8] I. Timor-Tritsch, *et al.* "Classification of Human Fetal Movement," *American J. of Ob. & Gyn.*, vol. 26, no.1, pp: 70-77, 1976.

[9] V. V. Athani, Stepper motors: fundamentals, applications and design. *New Age International*, 1997.

[10] C. Yang, *et al.*, "A Pilot Study on Fetal Heart Rate Extraction from Wearable Abdominal Inertial Sensors," *IEEE Sensors J.*, vol. 19, no. 22, pp. 10773-10781, 15, 2019.